16th World Conference on Earthquake, 16WCEE 2017
Santiago Chile, January 9th to 13th 2017
Paper N° 1483 (Abstract ID)
Registration Code: S-P1463619895

EFFECTS OF CYCLIC SHEAR DIRECTION ON EARTHQUAKE-INDUCED PORE WATER PRESSURE AND SETTLEMENT OF CLAY LAYER

H. Matsuda[(1)], TT. Nhan[(2)], H. Sato[(3)]

[(1)] *Professor, Yamaguchi University, hmatsuda@yamaguchi-u.ac.jp*
[(2)] *Assistant Professor, Yamaguchi University, nhan@yamaguchi-u.ac.jp; Lecturer, Hue University, nhan_hueuni@yahoo.com*
[(3)] *Doctor student, Fukken Co. Ltd., f16624@fukken.co.jp*

Abstract

In this paper, normally consolidated specimens of Kaolinite clay, Tokyo bay clay and Kitakyushu clay were tested under undrained uni-directional and multi-directional cyclic simple shear. The effect of cyclic shear direction on the pore water pressure accumulation during undrained cyclic shear and on the settlement after cyclic shear were investigated by focusing on the normalized pore water pressure ratio (DU) and post-cyclic settlement in strain ($D\varepsilon$), which are defined as the ratio of those induced by multi-directional cyclic shear ($(U_{dyn}/\sigma'_{v0})_M$ and ε_M) to those induced by uni-directional one ($(U_{dyn}/\sigma'_{v0})_U$ and ε_U), and also focusing on the difference of pore water pressure ratio (ΔU) and post-cyclic settlement ($\Delta\varepsilon$), which are defined as the difference between $(U_{dyn}/\sigma'_{v0})_M$, ε_M and $(U_{dyn}/\sigma'_{v0})_U$, ε_U, respectively.

It is shown from the experimental results that for all specimens, DU and $D\varepsilon$ firstly reach their peaks (DU_{max} and $D\varepsilon_{max}$) at the shear strain amplitude of about γ_{DUmax} = 0.1% - 0.4% for U_{dyn}/σ'_{v0} and $\gamma_{D\varepsilon max}$ = 0.1% - 0.2% for ε, then decreasing to smaller values. For clays used in this study, plasticity index is in the range from I_p = 25.5 to 63.8, then the maximum normalized pore water pressure ratio increases from DU_{max} = 2.19 to 3.12, which is smaller than the maximum normalized post-cyclic settlement being from $D\varepsilon_{max}$ = 2.62 to 3.62. As to the difference of pore water pressure ratio and post-cyclic settlement, ΔU and $\Delta\varepsilon$ firstly increase with the shear strain amplitude up to their maximum value ($\Delta U_{\max}$ and $\Delta\varepsilon_{\max}$) and decrease. For the range of I_p from 25.5 to 63.8, $\Delta U_{\max}$ decreases from 0.34 to 0.20, being smaller than $\Delta\varepsilon_{\max}$ which also falls from 2.56% to 1.02%, respectively. Meanwhile the shear strain amplitude for these peak values increases from $\gamma_{\Delta Umax}$ = 0.3% to 1.2% and from $\gamma_{\Delta\varepsilon max}$ = 1.0% to 1.2%. Therefore, it is suggested that the higher the Atterberg's limit (plasticity index) of clay, the smaller the effect of cyclic shear direction on the pore water pressure and the settlement becomes.

Keywords: clay, cyclic simple shear, pore water pressure, settlement, undrained

1. Introduction

The accumulation of pore water pressure and the settlement of soil induced by cyclic loading are divided as those not leading to failure and leading to failure, in which earthquake-induced pore water pressure and settlement are categorized as the latter phenomenon [1]. During earthquakes, soil layers are subjected to multi-directional cyclic shear with different strain amplitudes and frequencies [2]. Figs. 1(a) and (b) show the orbit of acceleration and the shear strain at GL-16m depth in Port Island during Hyogo-ken Nanbu Earthquake 1995 [3]. It is seen in these figures that the ground is subjected to the multi-directional cyclic shear strain during earthquakes.

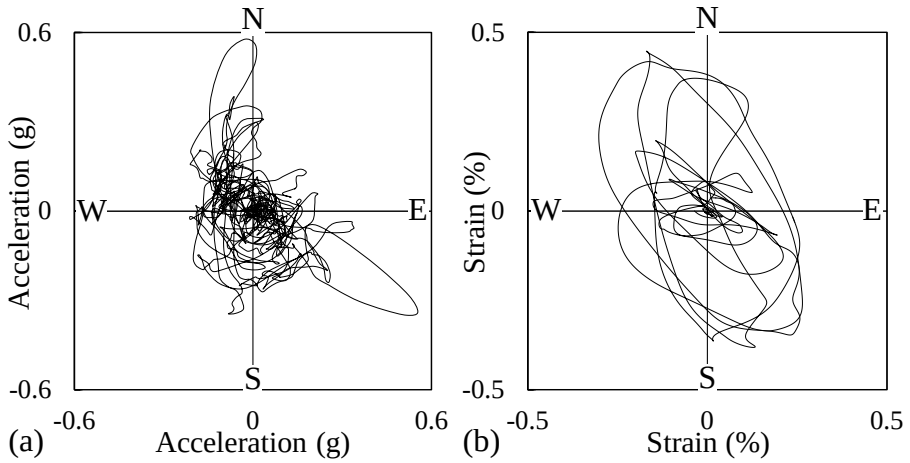

Fig. 1 – Orbit of (a) acceleration and (b) shear strain at Hyogo-ken Nanbu Earthquake 1995 [3]

Because of the short-term cyclic loading by an earthquake and/or the low permeability, the clay layer is under the undrained condition. Then the cyclic shear-induced pore water pressure increases gradually. The dissipation of cyclic shear-induced pore water pressure in the recompression stage after cyclic shear results in the instantaneous and long-term settlements which have been observed as a post-earthquake settlement after major earthquakes, such as Mexico Earthquake in 1985 [4], Hyogo-ken Nanbu Earthquake in 1995 [3] or the Tohoku Earthquake in 2011 [5]. When comparing the earthquake resistance of saturated clay with sand, soft cohesive soils are believed to be relatively stable because no liquefaction takes place even under strong motion by earthquakes [6, 7]. Consequently, the problems relating to the cyclic shear-induced pore water pressure and post-earthquake settlement for clay and sand are in the different situations. The effect of cyclic shear direction on the dynamic property of clays has been firstly pointed out on Boston blue clay by DeGroot *et al*. [8] and observed on Kaolinite clay by Matsuda *et al*. [9, 10], meanwhile these effects on the dynamic property of granular materials have been confirmed by many researches and taken into account in a long history.

Therefore, in this paper, normally consolidated specimens of Kaolin, Tokyo bay clay and Kitakyushu clay with different Atterberg's limit (plasticity index) were examined by using the multi-directional cyclic simple shear apparatus under the undrained condition followed by drainage. Then the effects of cyclic shear direction on the pore water pressure accumulation and on the settlement after cyclic shear were observed by focusing on the Atterberg's limit (plasticity index) of each clay.

2. Apparatus, specimens and test procedure

Figs. 2(a) and (b) show the photo and outline of the multi-directional cyclic simple shear test apparatus. This apparatus can apply any types of cyclic displacement at the bottom of specimen from two orthogonal directions by the electro-hydraulic servo system. Then a pre-determined vertical stress is also applied to the specimen by the aero-servo system. The shear box is the Kjellman type in which the specimen is enclosed in a rubber membrane. The flank of the membrane-enclosed specimen is surrounded by a stack of acrylic rings each of

which is 75.4 mm in inside diameter and 2 mm in thickness. By these stacked arcylic rings, the specimen is prevented from the lateral deformation but permitted to the cyclic simple shear deformation.

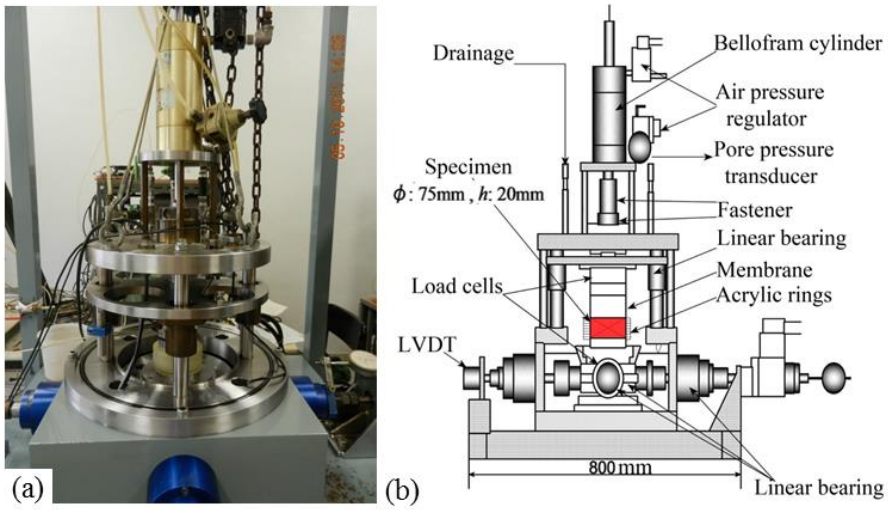

Fig. 2 – (a) Photo and (b) outline of the multi-directional cyclic simple shear test apparatus

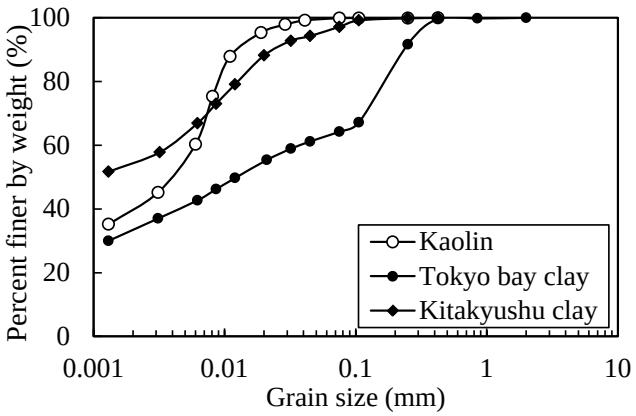

Fig. 3 – Grain size distribution of soils

Table 1 – Index properties of soils

Property	Kaolin	Tokyo bay clay	Kitakyushu clay
Specific gravity, G_s	2.71	2.77	2.63
Liquid limit, w_L (%)	47.8	66.6	98.0
Plastic limit, w_P (%)	22.3	25.0	34.2
Plasticity index, I_p	25.5	41.6	63.8
Compression index, C_c	0.31	0.46	0.60

The soils used in this study are Kaolinite clay, Tokyo bay clay and Kitakyushu clay. The grain size distribution curves and index properties of these soils are shown in Fig. 3 and Table 1, respectively. In order to

prepare the test specimen, samples were firstly mixed with de-aired water to form slurries having a water content of about $1.5 \times w_L$, and then each soil was kept in a big tank under the constant water content. Secondly, the slurry of each clay was de-aired in the vacuum cell. Thirdly, the slurry was poured into the shear box of the test apparatus and pre-consolidated under the vertical stress σ_{v0} = 49 kPa until the pore water pressure at the bottom surface of the specimen is confirmed to be dissipated. After the pre-consolidation, the dimension of specimen is 75 mm in diameter and about 20 mm in height and the initial void ratio (e_0) was about e_0 = 1.11-1.19, 1.20-1.37 and 1.61-1.81 for Kaolin, Tokyo bay clay and Kitakyushu clay, respectively. To satisfy the saturation of specimen in the undrained cyclic shear test, the pore pressure coefficient was confirmed to be higher than 0.95.

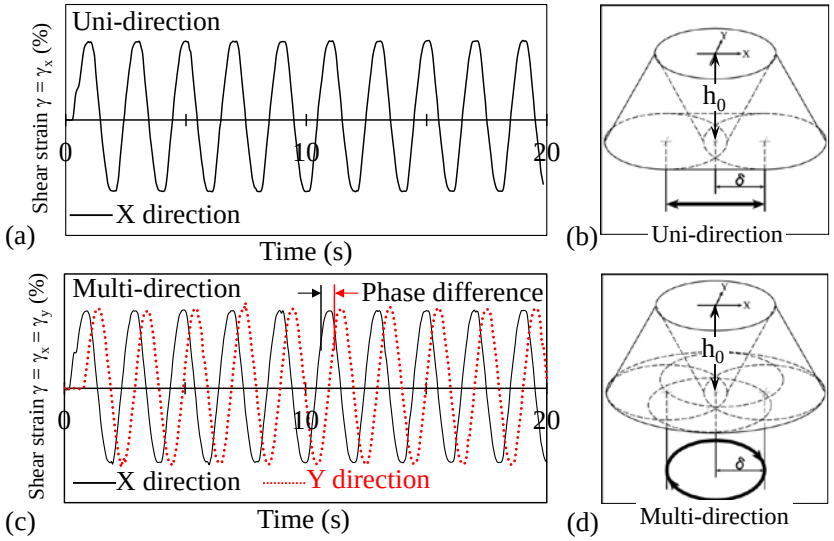

Fig. 4 – (a, c) Typical records of cyclic shear strains and (b, d) the respective deformations of specimen under uni-directional and multi-directional cyclic shear

Table 2 – Conditions of uni-directional and multi-directional cyclic simple shear tests

Period T (s)	Soil	Number of cycles n	Shear strain amplitude γ (%)
2	Kaolin	200	0.1, 0.2, 0.3, 0.4, 0.5, 0.6, 0.8, 1.0, 1.2, 2.0
		100	0.1, 0.4, 1.0, 1.2, 2.0
		50	0.1, 0.4, 1.0, 1.2, 2.0
		10	0.4, 1.0, 2.0, 3.0
	Tokyo bay clay	200	0.1, 0.2, 0.4, 0.8, 1.0, 1.2, 2.0
	Kitakyushu clay	200	0.1, 0.2, 0.4, 0.8, 1.0, 1.2, 2.0

After pre-consolidation is completed, the soil specimen was subjected to the strain-controlled cyclic simple shear under the undrained condition with pre-determined cyclic shear direction, shear strain amplitude (γ) and number of cycles (n). Following the undrained cyclic shear, the drainage from the top surface of the specimen was allowed and the cyclic shear-induced pore water pressure was fully dissipated and at the same time the settlement was measured with time. Figs. 4(a)-(d) show the typical records of cyclic shear strains and the deformation modes of specimen for the uni-directional and multi-directional cyclic shear, respectively. The shear strain amplitude γ is defined as a ratio of the maximum horizontal displacement (δ) to the initial height (h_0)

of specimen (Figs. 4b and d). In the uni-directional test, the cyclic shear strain was applied to the specimen only in X direction ($\gamma = \gamma_x$) (Figs. 4a and b) and so the orbit of cyclic shear strain forms a linear line (Fig. 4b). In multi-directional test (Figs. 4c and d), the cyclic shear strain was applied to the specimen in X direction (γ_x) and Y direction (γ_y), simutaneously which are perpendicular to each other under the same shear strain amplitude ($\gamma = \gamma_x = \gamma_y$) but with various phase differences (θ). Then the orbit shows an elliptical line for $0^0 < \theta < 90^0$ and a circle line for $\theta = 90^0$ which is well known as a gyratory cyclic shear (Fig. 4d). A series of experiments were carried out as shown in Table 2. The wave form of the cyclic shear strain was sinusoidal (two way cyclic strain) with the period T = 2 s and the amplitude was changed in the range from γ = 0.1% to 3.0%. The number of cycles was fixed as n = 10, 50, 100 and 200. For the multi-directional tests, the phase difference was changed as $\theta = 20^0$, 45^0, 70^0 and 90^0.

3. Test results and discussions

3.1 Pore water pressure accumulation and settlement of clays subjected to undrained uni-directional and multi-directional cyclic shear

As a result of the undrained cyclic shear, pore water pressure (U_{dyn}) increases with the number of cycles. Typical changes of the pore water pressure ratio which is defined by U_{dyn}/σ'_{v0}, during undrained uni-directional and multi-directional cyclic shear with different shear strain amplitudes are shown in Figs. 5(a)-(c) for Kaolin, Tokyo bay clay and Kitakyushu clay. Where σ'_{v0} is the initial effective stress and the observed results of uni-directional tests in these figures are notified as "uni". It is shown in these figures that U_{dyn}/σ'_{v0} increases with n and at the same value of n, the larger the shear strain amplitude γ, the higher the U_{dyn}/σ'_{v0} increases. In addition, at the same value of γ, U_{dyn}/σ'_{v0} induced by multi-directional cyclic shear is significantly larger than those generated by the uni-directional one. Similar tendencies are also seen for other values of γ as shown in Fig. 6(a), in which the relations between U_{dyn}/σ'_{v0} and γ under uni-directional and multi-directional cyclic shear are shown for each clay. For saturated sands, Matsuda *et al*. [11, 12] indicated that when $\gamma \geq$ 0.3%, the effective stress reduction ratio induced by uni-directional cyclic shear equals to those induced by multi-directional one and so the effect of cyclic shear direction becomes negligible when $\gamma \geq$ 0.3%. Meanwhile, the data in Figs. 5 and 6(a) show that the effect of cyclic shear direction on the pore water pressure accumulation of clays is evident for the range of shear strain amplitude from γ = 0.1% to 2.0%. In addition, when comparing the results for each clay, the higher the Atterberg's limit (plasticity index) of the soil, the slower the rate of pore water pressure accumulation (Fig. 5) leading to the lower pore water pressure in Kitakyushu clay and Tokyo bay clay, compared with those in Kaolinite clay (Fig. 6a). For the case of γ = 0.1% in Fig. 5, the pore water pressures on Kaolin evidently increase after several cycles of cyclic shear, while those on Tokyo bay clay and Kitakyushu clay fluctuate around zero even after a long-term application of cyclic shear strain.

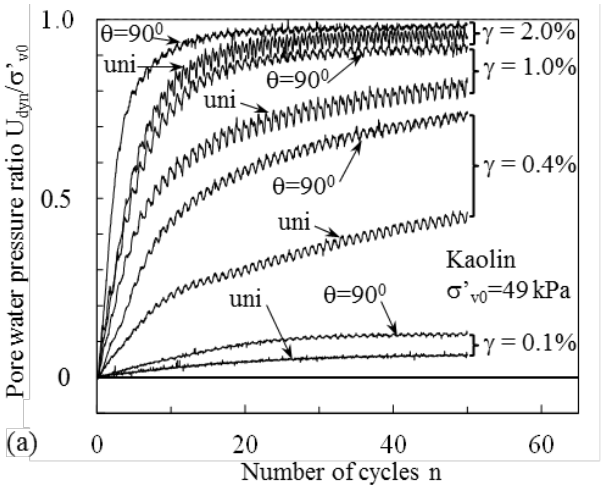

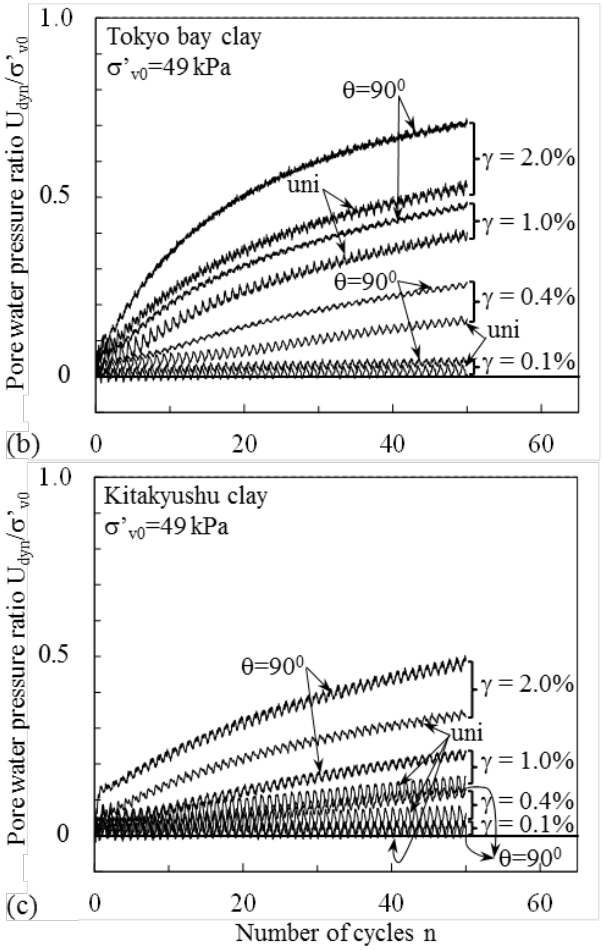

Fig. 5 – Typical changes of U_{dyn}/σ'_{v0} with n for (a) Kaolin, (b) Tokyo bay clay and (c) Kitakyushu clay during undrained uni-directional and multi-directional cyclic shear ($\theta = 90^0$)

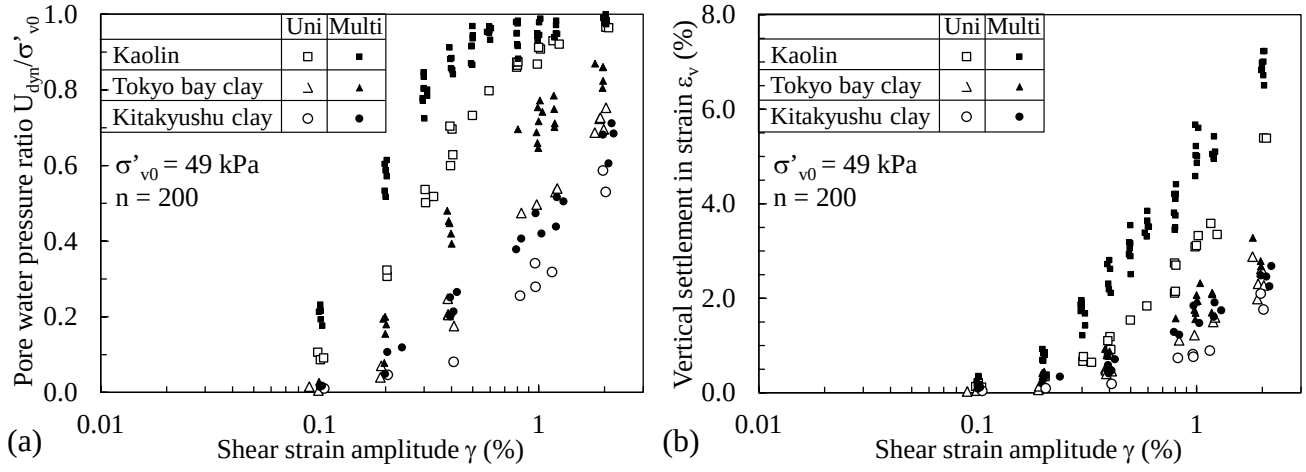

Fig. 6 – Changes of (a) U_{dyn}/σ'_{v0} and (b) ε_v with γ for clays subjected to undrained uni-directional and multi-directional cyclic shear

The relationships between the post-cyclic settlement ε_v and γ are shown in Fig. 6(b) for Kaolin, Tokyo bay clay and Kitakyushu clay subjected to uni-directional and multi-directional cyclic shear with n = 200. It is seen

in this figure that ε_v increases with γ and at the same γ, ε_v induced by multi-directional cyclic shear increases considerably larger than those induced by the uni-directional one and such a tendency is seen for all clays with a wide range of of Atterberg's limits (plasticity indices). In addition, results indicate that the soil with higher plasticity index shows the lower level of ε_v. Therefore, these observations suggest the significant effect of cyclic shear direction and the Atterberg's limit (plasticity index) of clay on the cyclic shear-induced pore water pressure and settlement in cohesive soils.

3.2 Normalized pore water pressure ratio and post-cyclic settlement in relation to plasticity index

In order to clarify the effect of cyclic shear direction on the cyclic shear-induced pore water pressure and on the settlement after cyclic shear, the normalized pore water pressure ratio DU and post-cyclic settlement $D\varepsilon$ are used. These parameters are defined as the ratio of pore water pressure ratio and settlement induced by multi-directional cyclic shear ($(U_{dyn}/\sigma'_{v0})_M$ and ε_M) to those induced by uni-directional one ($(U_{dyn}/\sigma'_{v0})_U$ and ε_U) and expressed by Eqs. (1) and (2) as follows:

$$DU = (U_{dyn}/\sigma'_{v0})_M / (U_{dyn}/\sigma'_{v0})_U \quad (1)$$

$$D\varepsilon = \varepsilon_M / \varepsilon_U \quad (2)$$

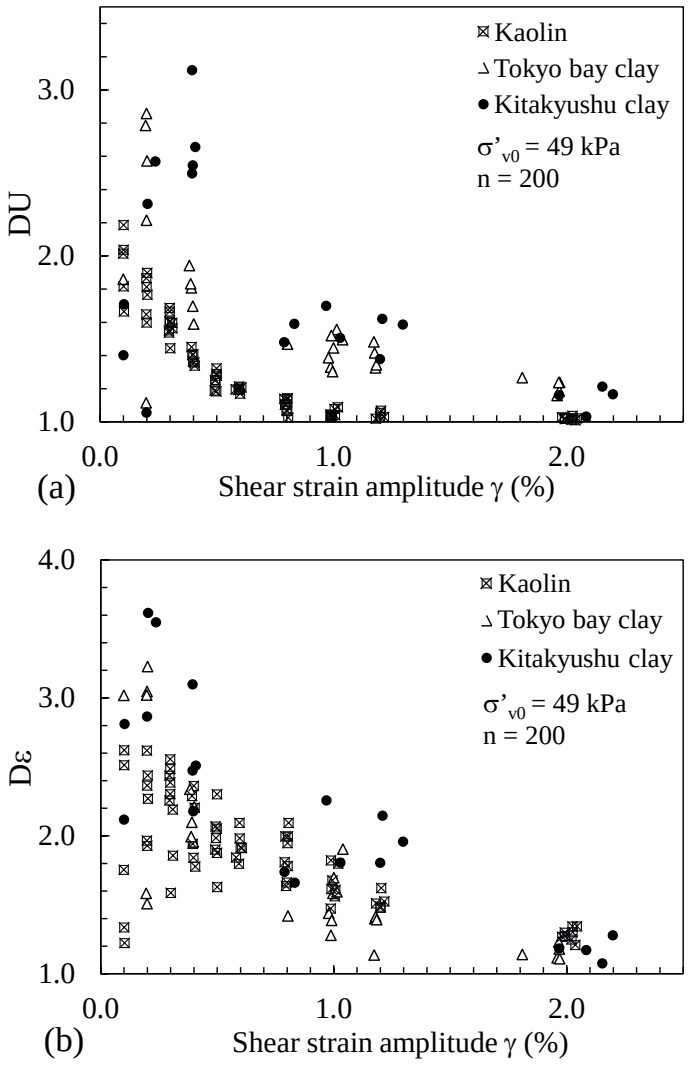

Fig. 7 – Changes of DU and $D\varepsilon$ with γ for clays subjected to uni-directional and multi-directional cyclic shear

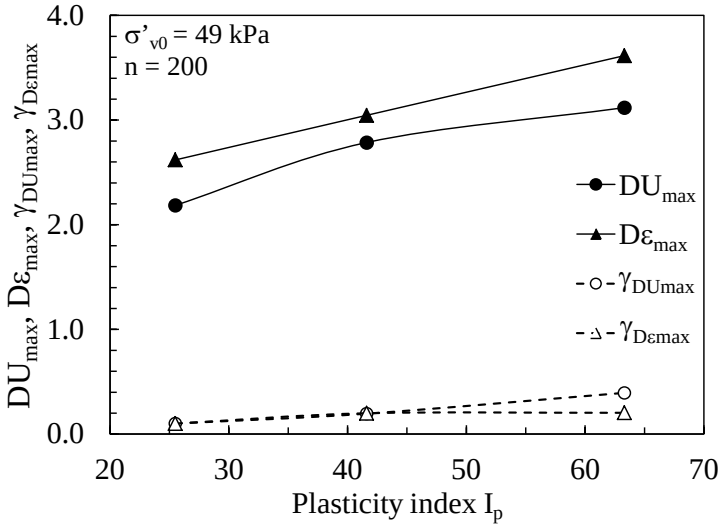

Fig. 8 – Changes of DU_{max}, $D\varepsilon_{max}$, γ_{DUmax} and $\gamma_{D\varepsilon max}$ with I_p

Figs. 7(a) and (b) show the changes of DU and $D\varepsilon$ with γ for Kaolin, Tokyo bay clay and Kitakyushu clay subjected to undrained uni-directional and multi-directional cyclic shear at n = 200. It is seen that DU and $D\varepsilon$ firstly reach their peaks (DU_{max} and $D\varepsilon_{max}$) at the shear strain amplitude of about γ_{DUmax} = 0.1% - 0.4% and $\gamma_{D\varepsilon max}$ = 0.1% - 0.2%, then decreasing (the shear strain amplitudes at which DU and $D\varepsilon$ reach their maximum DU_{max} and $D\varepsilon_{max}$ are denoted herein as γ_{DUmax} and $\gamma_{D\varepsilon max}$, respectively). Relationships between DU_{max}, $D\varepsilon_{max}$, γ_{DUmax}, $\gamma_{D\varepsilon max}$ and I_p are shown in Fig. 8. Based on the results of undrained uni-directional and multi-directional cyclic shear for the wide range of γ and n, Nhan *et al.* [13] indicated that the values of DU_{max}, $D\varepsilon_{max}$, γ_{DUmax} and $\gamma_{D\varepsilon max}$ are almost unchanged in the range of n from 10 to 200, meanwhile the increasing tendencies of DU_{max} and $D\varepsilon_{max}$ with Atterberg's limit (plasticity index) can be confirmed in Fig. 8.

3.3 Effect of cyclic shear direction regarding the differences of pore water pressure and post-cyclic settlement

3.3.1 Differences of pore water pressure ratio and settlement in relation to the number of cycles

The differences of pore water pressure ratio (ΔU) and post-cyclic settlement ($\Delta\varepsilon$) are plotted against γ in Figs. 9 and 10 for Kaolinite clay subjected to uni-directional and multi-directional cyclic shear with different n. These parameters are defined as the difference between $(U_{dyn}/\sigma'_{v0})_M$, ε_M and $(U_{dyn}/\sigma'_{v0})_U$, ε_U, respectively and expressed by Eqs. (3) and (4) as follows:

$$\Delta U = (U_{dyn}/\sigma'_{v0})_M - (U_{dyn}/\sigma'_{v0})_U \quad (3)$$

$$\Delta\varepsilon = \varepsilon_M - \varepsilon_U \quad (4)$$

It is seen in Figs. 9 and 10 that ΔU and $\Delta\varepsilon$ firstly increase with γ and reach their maximum (ΔU_{max} and $\Delta\varepsilon_{max}$), then consecutively decreasing. The values of ΔU_{max} and $\Delta\varepsilon_{max}$ and their corresponding shear strain amplitude, $\gamma_{\Delta Umax}$ and $\gamma_{\Delta\varepsilon max}$, are plotted against n in Fig. 11 (the shear strain amplitudes at which ΔU and $\Delta\varepsilon$ reach their maximum ΔU_{max} and $\Delta\varepsilon_{max}$ are denoted herein as $\gamma_{\Delta Umax}$ and $\gamma_{\Delta\varepsilon max}$). It is seen in this figure that, in the range of n = 10 to 200, ΔU_{max} and $\Delta\varepsilon_{max}$ increase from 0.24 to 0.34 and from 1.3% to 2.6%, meanwhile $\gamma_{\Delta Umax}$ and $\gamma_{\Delta\varepsilon max}$ decrease from 0.8% to 0.3% and from 3.0% to 1.0%, respectively. Therefore, these results suggest that the more the number of cycles, the larger the effect of cyclic shear direction on the pore water pressure accumulation and post-cyclic settlement, and that smaller amplitudes of cyclic shear strain are required for obtaining the maximum difference of pore water pressure ratio (ΔU_{max}) and settlement ($\Delta\varepsilon_{max}$) when the number of cycles increases.

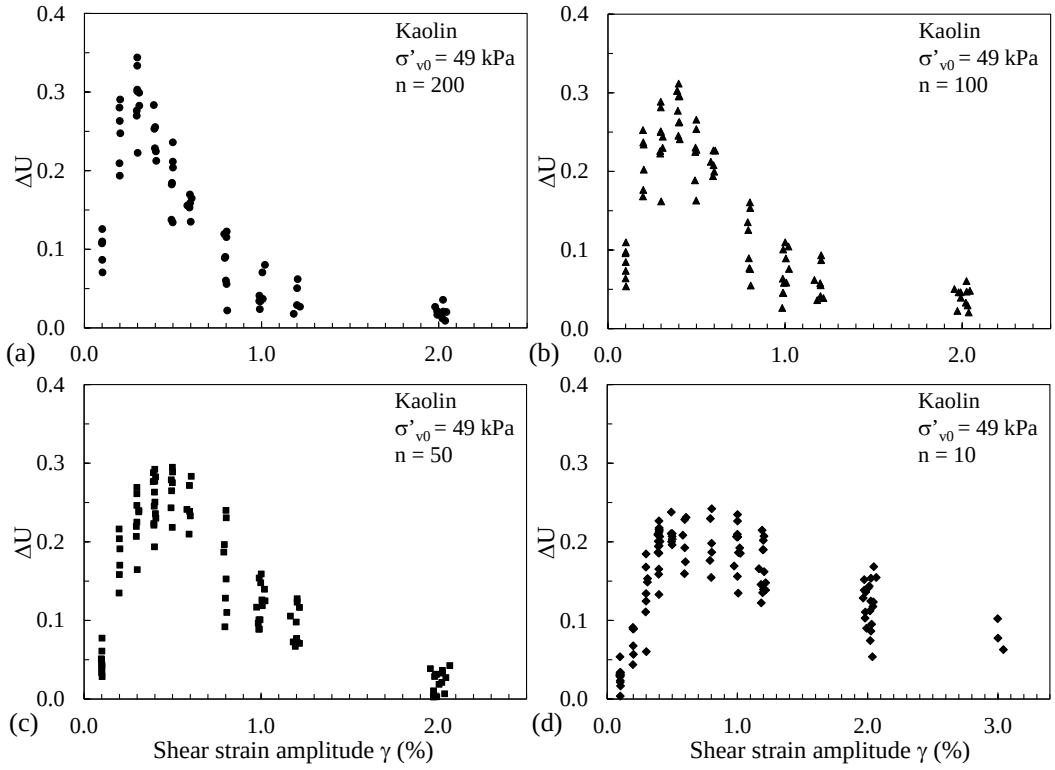

Fig. 9 – Changes of ΔU with γ for Kaolin subjected to undrained uni-directional and multi-directional cyclic shear at different n

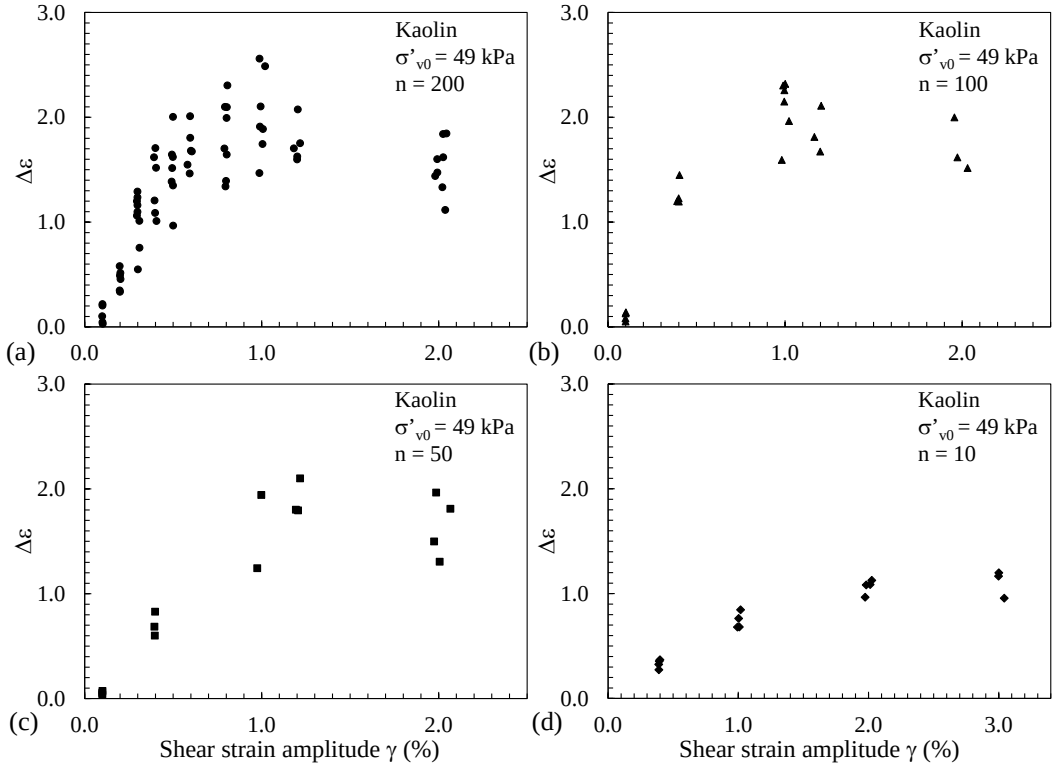

Fig. 10 – Changes of $\Delta\varepsilon$ with γ for Kaolin subjected to undrained uni-directional and multi-directional cyclic shear at different n

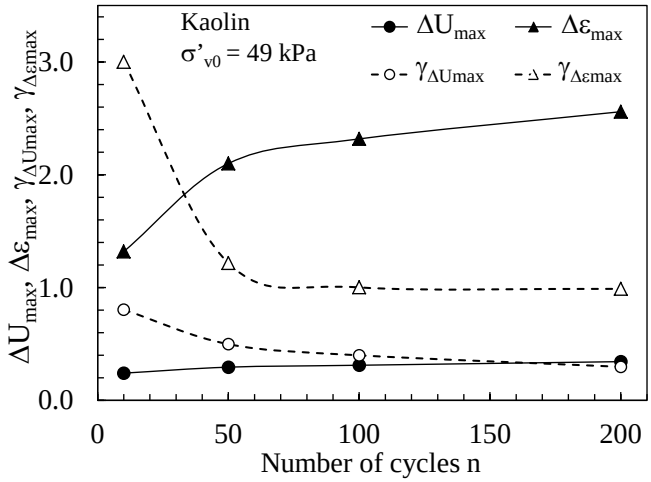

Fig. 11 – Changes of ΔU_{max}, $\Delta\varepsilon_{max}$, $\gamma_{\Delta Umax}$ and $\gamma_{\Delta\varepsilon max}$ with n for Kaolin subjected to undrained uni-directional and multi-directional cyclic shear

3.3.2 Differences of pore water pressure ratio and settlement in relation to plasticity index

The changes of ΔU and $\Delta\varepsilon$ with γ are shown in Figs. 12(a) and (b) for clays with different Atterberg's limits (plasticity indices). Similar to the tendency in Figs. 9 and 10, ΔU and $\Delta\varepsilon$ firstly increase with γ and reach their maximum, ΔU_{max} and $\Delta\varepsilon_{max}$, at a certain value of $\gamma_{\Delta Umax}$ and $\gamma_{\Delta\varepsilon max}$. In Fig. 13, when comparing the results on clays with different Atterberg's limits (plasticity indices), it is indicated that the changes of ΔU_{max}, $\Delta\varepsilon_{max}$, $\gamma_{\Delta Umax}$ and $\gamma_{\Delta\varepsilon max}$ with I_p are opposite to those with n (Fig. 11) and that, for the range of I_p from 25.5 to 63.8, ΔU_{max} and $\Delta\varepsilon_{max}$ decrease from 0.30 to 0.20 and from 2.6% to 1.0%, meanwhile $\gamma_{\Delta Umax}$ and $\gamma_{\Delta\varepsilon max}$ increase from 0.3% to 1.2% and from 1.0% to 1.2%, respectively. Therefore, the clay with higher Atterberg's limit (plasticity index) seems to undergo the smaller effect of cyclic shear direction when subjected to undrained multi-directional cyclic shear. Also, the shear strain amplitude required for these effects seem to be larger on the soil with higher Atterberg's limit (plasticity index).

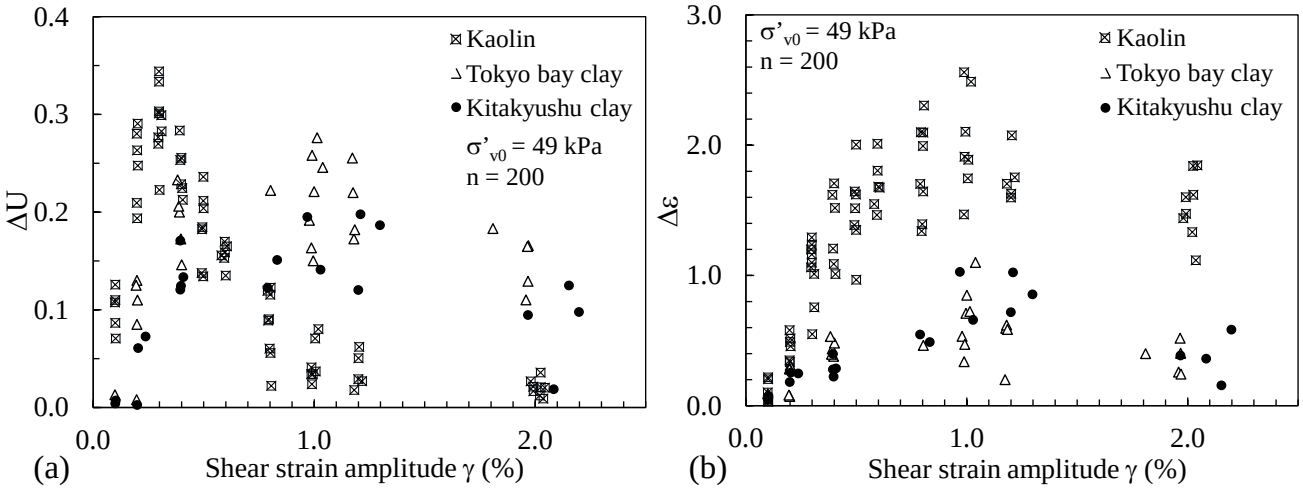

Fig. 12 – Changes of ΔU and $\Delta\varepsilon$ with γ for clays subjected to uni-directional and multi-directional cyclic shear

For Kaolinite clay with low Atterberg's limit (plasticity index), $\Delta\varepsilon_{max}$ and $\gamma_{\Delta\varepsilon max}$ are considerably higher than ΔU_{max} and $\gamma_{\Delta Umax}$ and these differences remain for a wide range of n (Fig. 11). Meanwhile for Tokyo bay

clay and Kitakyushu clay with higher Atterberg's limit (plasticity index), the differences between ΔU_{max} and $\Delta\varepsilon_{max}$ become smaller and $\gamma_{\Delta Umax}$ becomes equal to $\gamma_{\Delta\varepsilon max}$ as shown in Fig. 13.

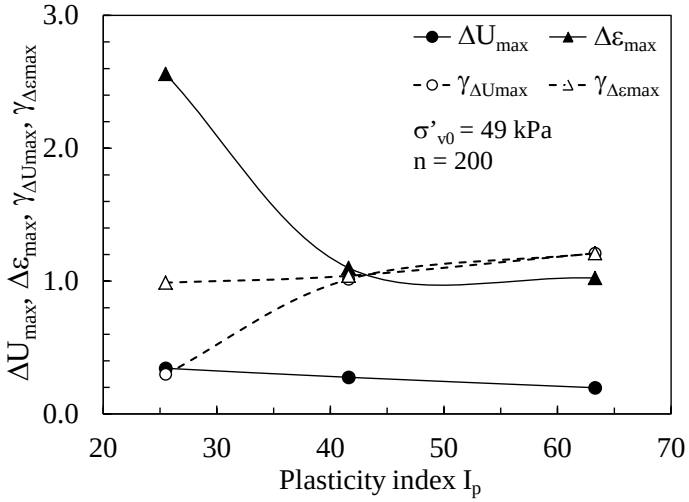

Fig. 13 – Tendency of ΔU_{max}, $\Delta\varepsilon_{max}$, $\gamma_{\Delta Umax}$ and $\gamma_{\Delta\varepsilon max}$ with I_p

4. Conclusions

Normally consolidated specimens of clays with a wide range of Atterberg's limits (plasticity indices) were tested by using the multi-directional cyclic simple shear test apparatus under undrained condition followed by drainage. The effects of cyclic shear direction on the pore water pressure accumulation and the settlement were then investigated. The main conclusions are as follows:

The effects of cyclic shear direction on the pore water pressure accumulation and the post-cyclic settlement are affected by the Atterberg's limit (plasticity index) of clay.

The maximum normalized pore water pressure ratio and settlement are almost constant in the range of n = 10 to 200 but becomes larger when the Atterberg's limit (plasticity index) of clay increases. In addition, the shear strain amplitudes for these maximum values are unchanged regardless of n and I_p.

The maximum differences of pore water pressure ratio and settlement increase with n but decrease with I_p. The shear strain amplitude for these maximum value shows opposite tendencies: $\gamma_{\Delta Umax}$ and $\gamma_{\Delta\varepsilon max}$ decrease with n but increase with I_p.

5. Acknowledgements

A part of this study was supported by National Foundation for Science and Technology Development of Vietnam (NAFOSTED) under Grant number 105.99-2014.04 and also by JSPS KAKENHI Grant Number 16H02362. The experimental works were also supported by the students who graduated Yamaguchi University. The authors would like to express their gratitude to them.

6. References

[1] Yasuhara K (1995): Consolidation and settlement under cyclic loading. *International Symposium on Compression and Consolidation of Clayey Soils*, Hiroshima, Japan.

[2] Ansal A, Iyisan R, Yildirim H (2001): The cyclic behavior of soils and effects of geotechnical factors in microzonation. *Soil Dynamics and Earthquake Engineering*, **21** (5), 445-452.

[3] Matsuda H, Shinozaki H, Okada N, Takamiya K, Shinyama K (2004): Effects of multi-directional cyclic shear on the post-earthquake settlement of ground. *13th World Conference on Earthquake Engineering*, Vancouver, Canada.

[4] Ohmachi T, Kawamura M, Yasuda S, Mimura C, Nakamura Y (1988): Damage due to the 1985 Mexico Earthquake and the ground conditions. *Soils and Foundations*, **28** (3), 149-159.

[5] Konagai K, Kiyota T, Suyama S, Asakura T, Shibuya K, Eto, C (2013): Maps of soil subsidence for Tokyo bay shore areas liquefied in the March 11th, 2011 off the Pacific Coast of Tohoku Earthquake. *Soil Dynamics and Earthquake Engineering*, **53**, 240-253.

[6] Yasuhara K, Hirao K, Hyde AFL (1992): Effects of cyclic loading on undrained strength and compressibility of clay. *Soils and Foundations*, **32** (1), 100-116.

[7] Yasuhara K, Murakami S, Toyota N, Hyde AFL (2001): Settlements in fine-grained soils under cyclic loading. *Soils and Foundations*, **41** (6), 25-36.

[8] DeGroot DJ, Ladd CC, Germaine JT (1996): Undrained multidirectional direct simple shear behavior of cohesive soil. *Journal of Geotechnical Engineering - ASCE*, **122** (2), 91-98.

[9] Matsuda H, Nhan TT, Ishikura R (2013): Excess pore water pressure accumulation and recompression of saturated soft clay subjected to uni-directional and multi-directional cyclic simple shears. *Earthquake and Tsunami*, **7** (4), 1-22.

[10] Matsuda H, Nhan TT, Ishikura R (2013): Prediction of excess pore water pressure and post-cyclic settlement on soft clay induced by uni-directional and multi-directional cyclic shears as a function of strain path parameters. *Soil Dynamics and Earthquake Engineering*, **49**, 75-88.

[11] Matsuda H, Andre PH, Ishikura R, Kawahara S (2011): Effective stress change and post-earthquake settlement properties of granular materials subjected to multi-directional cyclic simple shear. *Soils and Foundations*, **51** (5), 873-884.

[12] Matsuda H, Nhan TT, Ishikura R, Inazawa T (2012): New criterion for the liquefaction resistance under strain-controlled multi-directional cyclic shear. *15th World Conference on Earthquake Engineering*, Lisboa, Portugal.

[13] Nhan TT, Matsuda H, Hara H, Sato H (2012): Normalized pore water pressure ratio and post-cyclic settlement of saturated clay subjected to undrained uni-directional and multi-directional cyclic shears. *10th Asian Regional Conference of IAEG*, Kyoto, Japan.